ISSN 2350-1022

International Journal of Recent Research in Mathematics Computer Science and Information Technology
Vol. 12, Issue 1, pp: (73-80), Month: April 2025 – September 2025, Available at: www.paperpublications.org

ANALYSIS OF A 2D SHALLOW WATER MATHEMATICAL FLOOD WAVE MODEL OF BUDALANG'I

[1]Stephen Musindayi Miheso, [2]Opiyo Richard

[1]Department of Pure and Applied Mathematics, Maseno University, Kenya

[2]Department of Pure and Applied Mathematics, Maseno University, Kenya

DOI: https://doi.org/10.5281/zenodo.15737047

Published Date: 25-June-2025

Abstract: **This study focuses on analysis and evaluation of mathematical properties of 2D shallow water equations tailored to the Budalang'i floodplain. By applying the Froude number, the study identifies that supercritical flows are prevalent in the area. The model, derived from the 3D Navier-Stokes equations with the addition of a sink term, effectively captures the dynamics of the floodplain, highlighting the importance of this modification for accurate boundary condition representation. The study employed a finite difference scheme to solve the 2D shallow water equations. The results demonstrate that incorporating a sink term significantly improves the model's performance by achieving steady-state velocity, reducing high-frequency oscillations and turbulence, and mitigating over-bank flows. Although the Coriolis term was considered, it had a negligible impact on the flow state, underscoring that the sink term is the critical factor in enhancing flood control and providing valuable insights for flood management strategies.**

Keywords: **sink, Coriolis, Flood.**

1. INTRODUCTION

Mathematical modeling of flood propagation provides a precise quantitative description of how large volumes of water move across the earth's surface uncontrollably. This modeling considers external boundaries, internal geometry, boundary conditions, and flow terms to numerically approximate flood behavior in specific areas [2]. The goal is to develop a robust mathematical framework that employs algorithms to simulate flow dynamics effectively [3].

In flood modeling analysis, the focus is on the physical changes governed by fundamental laws, such as the Navier-Stokes equations. Due to their complexity, simplified models like the shallow water equations (SWE) are commonly used [3]. Significant advancements have been made in computational techniques to model various water flow phenomena, including flood waves, dam-breaks, and tidal flows [5]. This study aims to apply the 2D shallow water model to the Budalang'i floodplain in Busia County, Kenya, to provide a detailed and accurate simulation of flood propagation in the region.

Analyzing and simulating flood propagation in the Budalang'i floodplain is increasingly vital due to the growing risks posed by climate change, population expansion, and deforestation. Floods, which often occur suddenly and with severe intensity, present significant challenges for prediction systems, particularly in developing regions such as Kenya. The Budalang'i area has a history of devastating floods, including notable events in 1937, 1947, 1957, 1978, and 2002, which have led to considerable damage and widespread displacement [4].

From an analytical perspective, the focus is on exploring various flood modeling techniques, with particular emphasis on the 2D shallow water equations (SWE). These equations offer a framework for understanding shallow water flow dynamics, taking into account factors such as topography and friction [3]. Previous research has advanced 2D SWE models to address

ISSN 2350-1022

International Journal of Recent Research in Mathematics Computer Science and Information Technology
Vol. 12, Issue 1, pp: (73-80), Month: April 2025 – September 2025, Available at: www.paperpublications.org

issues such as viscous effects, drag terms, and varying topographies [10,7]. Despite these advancements, existing models often struggle to accurately predict flood wave dispersion and depth variations, especially in complex floodplain settings like Budalang'i. Attempts to simulate and analyse shallow water equations have been made. sophisticated computational techniques are utilized to model flood propagation effectively. These include methods such as finite volume techniques, high-resolution schemes, and Riemann solvers [6,8,12]. While these approaches have improved flood modeling, challenges persist in capturing intricate boundary conditions and simulating the full dynamics of wave dispersion and depth variations. Studies of flood modeling in Western Kenya highlight the necessity for precise flood wave predictions and underscore the limitations of current methods in fully representing flood events [9,1]. This study aims to bridge these gaps by applying the 2D SWE to the Budalang'i floodplain, striving to enhance flood propagation simulations and develop more effective tools for flood management and prediction.

2. MODEL ANALYSIS AND SIMULATION

The linearized shallow water equations are:

$$\frac{\partial \eta}{\partial t} + \frac{\partial u(\eta+h)}{\partial x} + \frac{\partial v(\eta+h)}{\partial y} = s_1 \quad (2.0.1)$$

$$\frac{\partial u}{\partial t} - fv = -g\frac{\partial \eta}{\partial x} \quad (2.0.2)$$

$$\frac{\partial v}{\partial t} + fu = -g\frac{\partial \eta}{\partial y} \quad (2.0.3)$$

Given $H = \eta + h$, we rewrite the shallow water equations (2.0.1) to (2.0.3) in primitive form:

$$\frac{\partial \eta}{\partial t} + \frac{\partial}{\partial x}[(\eta + h)u] + \frac{\partial}{\partial y}[(\eta + h)v] = 0 \quad (2.0.4)$$

$$\frac{\partial u}{\partial t} + u\frac{\partial u}{\partial x} + v\frac{\partial u}{\partial y} - fv + g\frac{\partial \eta}{\partial x} = 0 \quad (2.0.5)$$

$$\frac{\partial v}{\partial t} + u\frac{\partial v}{\partial x} + v\frac{\partial v}{\partial y} + fu + g\frac{\partial \eta}{\partial y} = 0 \quad (2.0.6)$$

To analyze flow stability, matrices A and B for conserved variables in the x and y directions, respectively, are formed using the Jacobian transformation:

$$A = \frac{\partial F(U)}{\partial U} = \begin{bmatrix} u & \eta + h & 0 \\ g & u & 0 \\ 0 & 0 & u \end{bmatrix}, \quad B = \frac{\partial G(U)}{\partial U} = \begin{bmatrix} v & 0 & \eta + h \\ 0 & v & 0 \\ g & 0 & v \end{bmatrix}$$

The eigenvalues of matrix A are determined by solving $|A - \lambda I| = 0$:

$$\begin{vmatrix} u - \lambda & \eta + h & 0 \\ g & u - \lambda & 0 \\ 0 & 0 & u - \lambda \end{vmatrix} = 0$$

Resulting in:

$$(u - \lambda)^2(u - \lambda) - (\eta + h)g(u - \lambda) = 0$$

Solving this, we find:

$$\lambda_1 = u, \quad \lambda_2 = u + \sqrt{g(\eta + h)}, \quad \lambda_3 = u - \sqrt{g(\eta + h)}$$

Similarly, for the y direction:

$$\lambda_1 = v, \quad \lambda_2 = v + \sqrt{g(\eta + h)}, \quad \lambda_3 = v - \sqrt{g(\eta + h)}$$

Corresponding eigenvectors in the x direction are:

$$r_1 = \begin{bmatrix} 1 \\ \lambda_1 \\ u \end{bmatrix}, \quad r_2 = \begin{bmatrix} 0 \\ 0 \\ 1 \end{bmatrix}, \quad r_3 = \begin{bmatrix} 1 \\ \lambda_3 \\ u \end{bmatrix}$$

And for the y direction:

$$r_1 = \begin{bmatrix} 1 \\ \lambda_1 \\ v \end{bmatrix}, \quad r_2 = \begin{bmatrix} 0 \\ 0 \\ 1 \end{bmatrix}, \quad r_3 = \begin{bmatrix} 1 \\ \lambda_3 \\ v \end{bmatrix}$$

These eigenvalues indicate that the shallow water equations are hyperbolic, admitting discontinuous weak solutions, such as bores or breaking waves. The Froude number, Fr, relates convective velocity to phase velocity, with $Fr > 1$ indicating supercritical flow:

$$Fr_x^2 = \frac{u^2}{gH}, \quad Fr_y^2 = \frac{u^2}{gH}$$

In Budalang'i flood plain, rapid surface waves during floods result in supercritical flows. The average discharge is 30, increasing to 90 during heavy rains, indicating $Fr_x^2 > 1$. The nonlinear terms are linearized for numerical simulation:

$$u = U + u', \quad v = V + v', \quad \eta = H + \eta'$$

Assuming $V = U = 0$ for mean flow, the analyzed and linearized shallow water equations become:

$$\frac{\partial \eta}{\partial t} + \frac{\partial u(\eta + h)}{\partial x} + \frac{\partial v(\eta + h)}{\partial y} = s_1 \tag{2.0.7}$$

$$\frac{\partial u}{\partial t} - fv = -g\frac{\partial \eta}{\partial x} \tag{2.0.8}$$

$$\frac{\partial v}{\partial t} + fu = -g\frac{\partial \eta}{\partial y} \tag{2.0.9}$$

The study aimed to characterize the Budalng'i shallow water flood waves through numerical simulations. The gravity waves generated by inflows from upstream rivers were simulated using a finite difference Mac Cormac scheme, which involved a predictor-corrector method. The domain was spatially discretized into cells indexed by (i, j), and finite difference methods were applied to solve the equations. Initially, the water height was non-uniform, with disturbances caused by inflow.

The Coriolis parameter f was assumed to be independent of geographical latitude, with $\beta = 0$. Gravity waves, known for their speed, required outputs every 30 minutes. The time step Δt was determined based on grid spacing and velocity components, ensuring stability through the Courant-Friedrichs-Lewy condition. Neumann boundary conditions were imposed, with velocity components at the boundary set to zero.

Parameters included an acceleration due to gravity of $9.81\ \mathrm{m/s^2}$, a small Coriolis parameter of 0.00005, a Manning's coefficient of 0.015, and a bed slope of 0.26%. These simulations provided insights into the behavior of shallow water models under these conditions.

3. RESULTS AND DISCUSSIONS

Figure 1 depicts the initial water inflow into the basin at the beginning of the long rains. Initially, small tributaries have little effect compared to the flooding, but as inflow increased, a wave pattern developed, indicating the spread of a gravity wave caused by disturbances in the basin. The vertical velocity of the water changed over time, eventually decreasing and dispersing in opposite directions from the initial disturbance.

The wave's development is time-dependent. Initially, the water is still, with boundaries set by the basin walls. Shortly after, the water begins moving in all directions, generating outward-propagating circular shock waves and inward-moving rarefaction waves that nearly reach the center. This continues until the rarefaction wave fully enters the center and is reflected, causing a sharp change in the water surface elevation, as shown in Figure 1.

International Journal of Recent Research in Mathematics Computer Science and Information Technology
Vol. 12, Issue 1, pp: (73-80), Month: April 2025 – September 2025, Available at: www.paperpublications.org

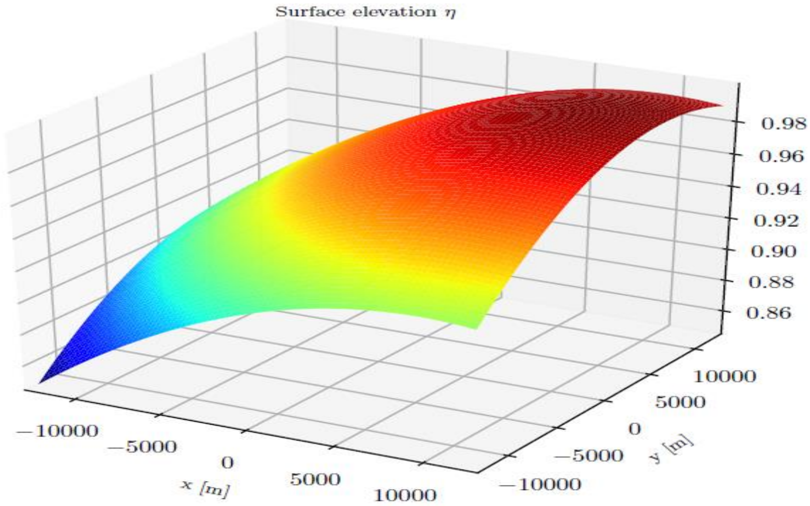

Figure 1: Initial wave

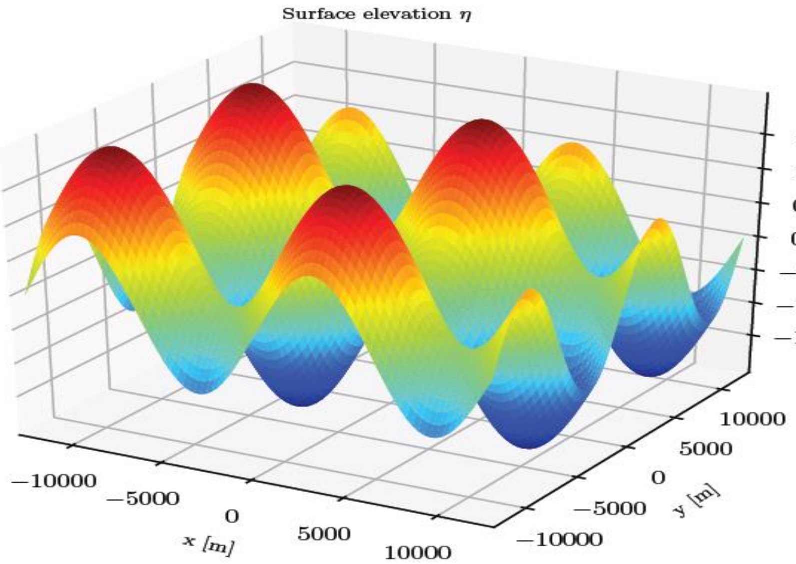

Figure 2: Turbulence

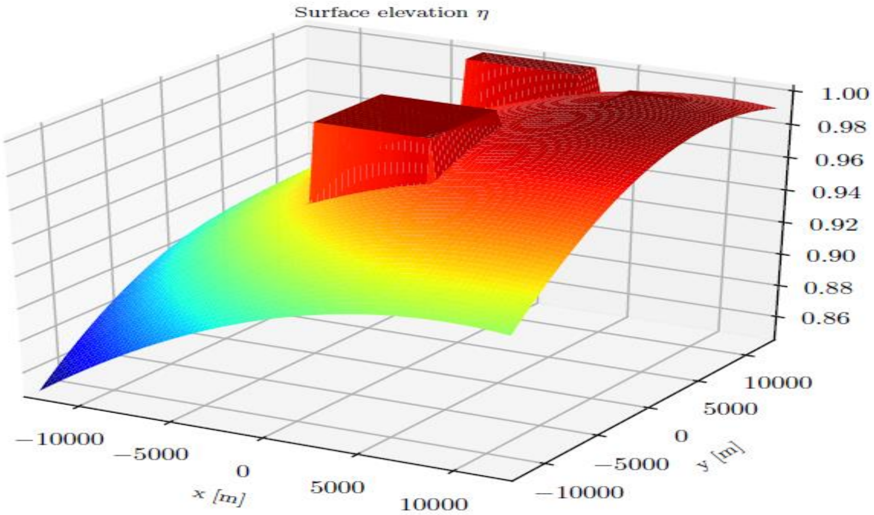

Figure 3: Overbank flow

International Journal of Recent Research in Mathematics Computer Science and Information Technology
Vol. 12, Issue 1, pp: (73-80), Month: April 2025 – September 2025, Available at: www.paperpublications.org

As the heavy rains continued, wave generation increased due to rising water levels. The wave propagation became unstable, leading to higher frequency and amplitude (Figure 2). This instability worsened by increased bottom friction from wave dispersion along the banks and previous sediment buildup. Consequently, the risk of the banks bursting grows, posing a threat to nearby areas due to submerged dykes (Figure 3).

The analysis suggests that the turbulence in the waves increases at the peak of inflow, indicating a higher likelihood of wave breaking and shocks during heavy rains (Figure 2). This turbulence, linked to high-frequency waves, appears to drive the flooding in the Budalang'i area. While the findings align with other experimental studies, achieving more accurate results is challenging due to the complex topography of the region, so only approximate conclusions specific to this area are presented.

Regarding flood prevention, dykes initially resist rising water levels during heavy downpours. However, due to earlier sediment buildup, floodwaters eventually overflow the dykes, leading to overbank bursts and rendering the dykes ineffective (Figure 3). This scenario underscores the importance of dykes in flood management, although their effectiveness is often temporary. The increased turbulence and energy of the shallow water waves further intensify this issue, contributing to the dykes' submersion (Figure 3).

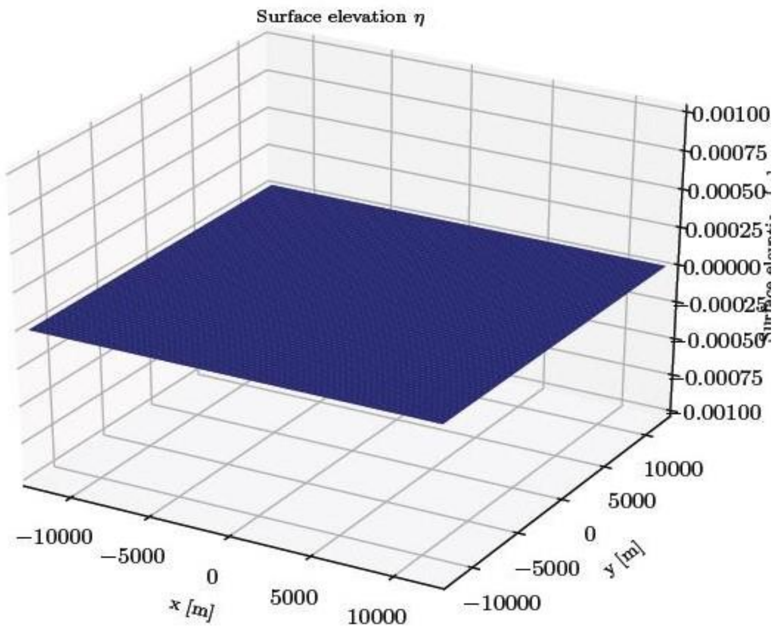

Figure 4: Sink

To mitigate this, a "sink" mechanism was introduced to represent the water that infiltrates underground or is absorbed by boreholes within the basin. This concept also extends to the sedimentation removed from the area, highlighting the persistent challenges in managing floodwaters and sediment in the region (Figure 4).

The implementation of a sink within the basin resulted in wave attenuation due to sediment extraction and reflection. This process caused a decrease in water volume and a progressive decline in wave turbulence (Figure 4). Although not visualized in Figure 4, the system ultimately tends toward a static condition. The sink's efficacy in controlling water levels suggests its potential for flood prevention in the region (Figure 4).

Over time, the primary circular shock wave expanded outward, with damping reducing its strength, while a secondary wave moved inward. As the primary wave neared the domain boundary, it created a small gradient in water surface elevation. The secondary waves' reflections led to a steady velocity state, with energy reduction weakening both wave types (Figure 5). To compare solutions, linearized shallow water equations were solved, incorporating Coriolis effects and Earth's rotation. The initial disturbance from water inflow generated waves, and velocities u and v led to gravity waves radiating outward, as depicted in Figure 5.

International Journal of Recent Research in Mathematics Computer Science and Information Technology
Vol. 12, Issue 1, pp: (73-80), Month: April 2025 – September 2025, Available at: www.paperpublications.org

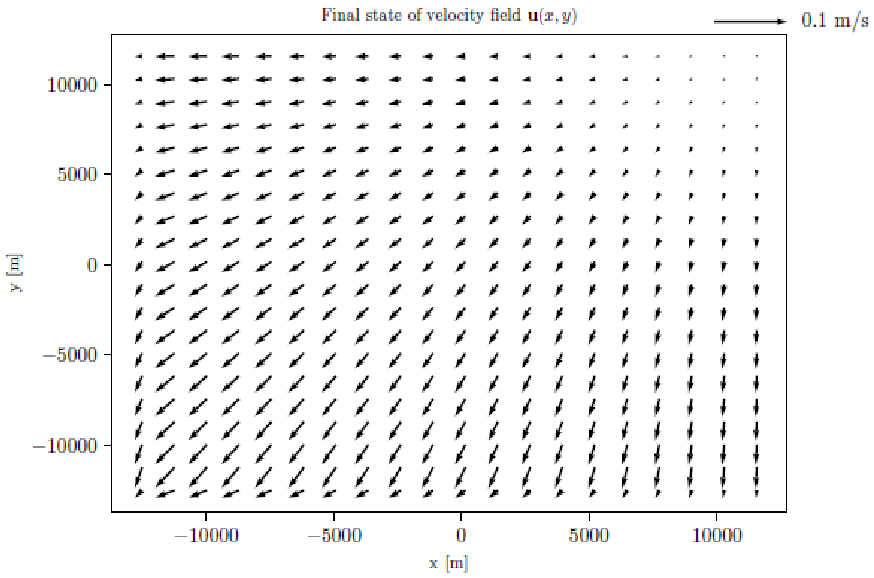

Figure 5: Steady state

The inclusion of the Coriolis term significantly impacts the turbulence, which is crucial for understanding geostrophic effects (Figure 6). Wave reflection is minimal, leading to the instability of gravity waves and eventual overbank flooding, causing damage to the surrounding area (Figure 6). The second snapshot of shallow water simulations shows wave disturbances similar to Coastal Kelvin and Rossby Waves, with the waves dissipating away from the disturbance. The boundary conditions, assumed to be zero (y = 0) due to dykes, result in an exponential decay of the waves as they move away from the source (Figure 6).

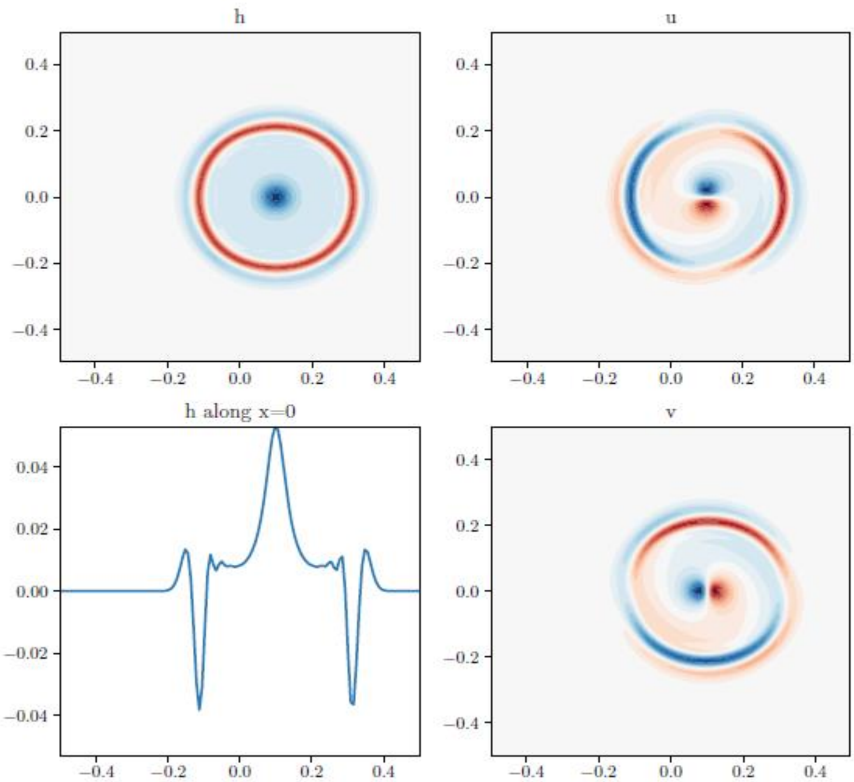

Figure 6: Coriolis term

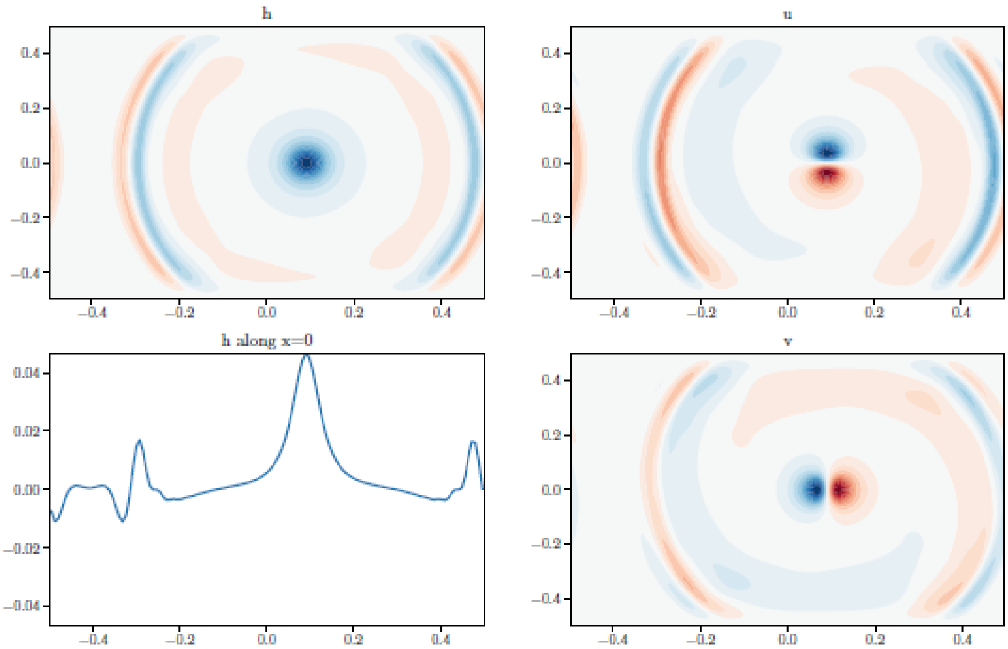

Figure 7: Wave decay

Over time, the wave begins to decay with varying behaviors (Figure 7). Although the wave continues to decay in opposite directions, there are signs of weak reflection as the days progress (Figure 7). The addition of a sink term to the model likely contributed to reduced energy and increased reflections, ultimately mitigating environmental damage (Figure 7). The study suggests that introducing a sink, such as regular maintenance of the floodplain by removing sediments, could be an economical solution. Alternatively, constructing a dam might also address the problem.

4. CONCLUSION

The analysis concluded that the Budalang'i floodplain experiences supercritical flows during heavy rainfall, characterized by high-velocity waves that cause significant disturbances in surrounding areas.Through simulation of the identified equations, results indicated that these supercritical flows are the primary drivers of turbulent and overbank flows. However, incorporating a sink term, such as a borehole, effectively controls and mitigates these issues.

5. ACKNOWLEDGMENT

The authors express their gratitude to Maseno University for its support, and to the reviewers for their valuable and constructive feedback. The authors also acknowledge the excellent work by Opiyo et al. [11], which served as a key source of inspiration for this study.

REFERENCES

[1] Bashar, K., Mutua, F., Mulungu, D., Deksyos, T., and Shamseldin, A. (2005). Appraisal study to select suitable rainfall-runoff model for the nile river basin. In *Proceedings of International Conference of UNESCO Nile Project*, page 1215.

[2] Bernadelli, H. (2003). Water waves. *Journal of the Burma Research Society*, 31:1–18.

[3] Bernadelli, H. (2013). Mathematical modeling techniques for flood propagation in urban areas. *Journal of the Burma Research Society*, 25:1–4.

[4] Bloch, I., Jean, D., and Sylvain, N. (2012). Quantum simulations with ultracold quantum gases. *Nature Physics*, 8:267–276.

ISSN 2350-1022

International Journal of Recent Research in Mathematics Computer Science and Information Technology
Vol. 12, Issue 1, pp: (73-80), Month: April 2025 – September 2025, Available at: www.paperpublications.org

[5] Delis, A. and Katsaounis, T. (2005). Numerical solution of the two-dimensional shallow water equations by the application of relaxation methods. *Applied Mathematical Modelling*, 8:754–783.

[6] Elena, M. (2009). The shallow water model: The relevance of geometry and turbulence. *Monographs of the Royal Academy of Sciences of Zaragoza*, 31:217–236.

[7] Ferrari, S. and Fausto, S. (2004). A new two-dimensional shallow water model including pressure effects and slow varying bottom topography. *ESAIM: Mathematical Modelling and Numerical Analysis*, 38:211–234.

[8] Hervouet, J. (2000). A high resolution 2d dam-break model using parallelization. *Hydro- logical Processes*, 6:2211–2230.

[9] Kiluva, V., Otengi, S., and Miima, J. (2018). Rainfall runoff modelling in river yala basin, western kenya. *Journal of Science Technology Education and Management*, 20:21–28.

[10] Marche, F. (2007). Derivation of a new two-dimensional viscous shallow water model with varying topography, bottom friction and capillary effects. *European Journal of Mechanics- B/Fluids*, 26:20–31.

[11] Otieno, O. R. and Juma, O. M. (2025). Analysis of riga plates and magnetism inclination effects on temperature profile for unsteady mhd stokes flow of a dusty fluid. *International Journal of Recent Research in Mathematics Computer Science and Information Technology*, 11(2).

[12] Zoppou, P. (2007). Second-order approximate riemann solver with a van leer type limiter. *Biometrika*, 33:183–212.